Philippine Journal of Science
148 (1): 167-172, March 2019
ISSN 0031 - 7683
Date Received: 29 Oct 2018

RESEARCH NOTE

Effect of Solvent on Gd(DOTA)$^{-}$ Complex Formation: A Preliminary Investigation

Ernest Guiller S. Pineda and **Aaron Joseph L. Villaraza***

Institute of Chemistry, College of Science, University of the Philippines Diliman,
Quezon City, Metro Manila 1101 Philippines

The thermodynamic stability and kinetic inertness of gadolinium-based MRI contrast agents remains an important research topic in the field of radiological contrast agent development. In this study, the kinetics and thermodynamics of Gd^{3+}-complex formation with the macrocyclic ligand DOTA (*i.e.*, 1,4,7,10-tetraazacyclododecane-1,4,7,10-tetraacetic acid) was investigated under aqueous (acetate buffer pH 5.8) and non-aqueous (MeOH) conditions. Using Job's method of continuous variation, solutions were prepared of increasing mole fraction of Gd^{3+} relative to xylenol orange (XO, *i.e.*, 3,3′-bis[*N,N*-bis(carboxymethyl)aminomethyl]-o-cresolsulfonephthalein) in MeOH, and their absorbances were measured at 582 nm.The kinetics of complex formation *via* ligand substitution of DOTA and DO3A (*i.e.*, 1,4,7,10-tetraazacyclododecane-1,4,7-triacetic acid) with Gd-XO under aqueous and non-aqueous conditions were determined using UV-Vis spectrophotometry. Furthermore, the thermodynamic parameters of DOTA complexation with Gd^{3+} for both solvent conditions were compared by measuring the heats of injection using isothermal titration calorimetry. Results of this study demonstrate that XO forms a well-defined 1:1 stoichiometry with Gd^{3+} regardless of solvent polarity. Meanwhile, the rate of ligand substitution between Gd-XO and the macrocyclic ligand is effectively minimized under non-aqueous conditions ($k_{obs,\,buffer} = 33.9 \pm 1.0 \times 10^{-3}\ s^{-1}$; $k_{obs,MeOH} = 5.62 \pm 2.22 \times 10^{-3}\ s^{-1}$). The binding reaction of Gd^{3+} with DOTA has comparable negative ΔG values in the two solvents ($\Delta G_{buffer} = -9.28 \pm 0.57$ kcal/mol; $\Delta G_{MeOH} = -8.19 \pm 0.14$ kcal/mol), suggesting that the reaction is equally spontaneous under both conditions. However, computation of global thermodynamic properties demonstrate that the reaction is entropically-driven in acetate buffer in comparison with MeOH where the reaction is enthalpy-driven. Finally, the nature of solvent has an effect on the metal-to-ligand stoichiometry (*N*) of the resulting complex, which in acetate buffer (*N* = 1:1) is lower than that in MeOH (*N* = 1:2). These results are important in the context of optimizing reaction conditions in the preparation of related MRI contrast agents.

Key words: binding kinetics, calorimetry, gadolinium-based MRI contrast agents, isothermal titration ligand exchange reaction, solvent effects, thermodynamics

INTRODUCTION

The stability of Gd^{3+}-complexes with macrocyclic ligands in the context of radiologic contrast agent (CA) development for clinical use remains a topic of interest, as *in vivo* decomplexation of Gd^{3+} is associated not only with the onset of Nephrogenic System Fibrosis (NSF) but also with Gd^{3+} accumulation in the brain of healthy patients (Garcia *et al.* 2017).

A facile method for measuring the kinetics of Gd-complex formation in acetate buffer *via* ligand substitution had been reported using the Gd^{3+}-xylenol orange (Gd-XO) complex as a colorimetric probe (Suazo and Villaraza 2015); the

*Corresponding author: alvillaraza@up.edu.ph

rate at which the ligand exchange occurs is a function of ligand structure, denticity, and the nature of functional groups (Belleza *et al.* 2018).

$$\text{Gd-XO } (\textit{purple}) + \text{L} \rightarrow \text{Gd-L} + \text{XO } (\textit{yellow})$$

Considering however that studies which describe the preparation of such complexes are performed in a non-aqueous solvent such as methanol (MeOH) (for instance, Natrajan *et al.* 2009), we endeavored to see if the nature of solvent would also have an effect on the rate of complex formation.

Using Job's method of continuous variation (Job 1928), MeOH solutions were prepared of increasing mole fraction of Gd^{3+} (*i.e.*, X_{Gd}) relative to XO, and their absorbances measured at λ_{max} = 582 nm. The solution which exhibited the strongest absorption was observed at X_{Gd} = 0.5, indicating that in MeOH the stoichiometry of Gd^{3+} to XO is 1:1 (Fig. 1).

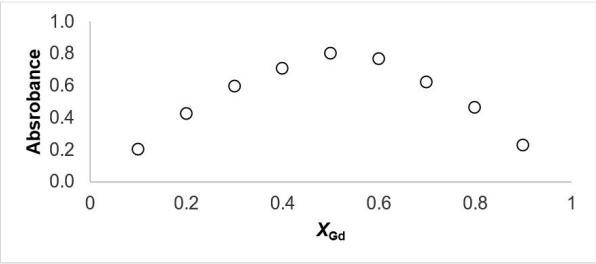

Figure 1. Job plot of Gd-XO in MeOH: absorbance at 582 nm is plotted against X_{Gd}

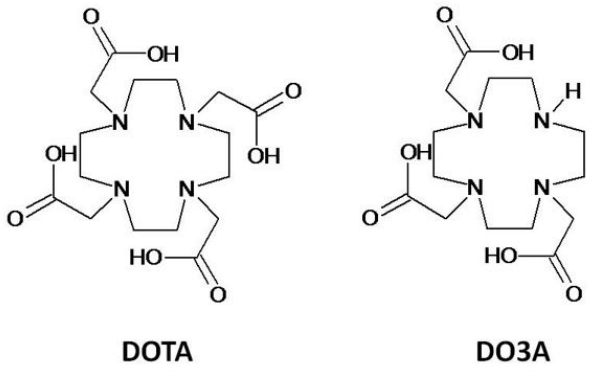

Figure 2. Macrocyclic ligands used in this study: octadentate DOTA and heptadentate DO3A.

In order to investigate the effect of solvent on the rate of metal complexation, the absorbance of Gd-XO in competition with the macrocyclic ligands DOTA and DO3A (Fig. 2) were measured in MeOH and acetate buffer as a function of time (Table 3).

Table 1. Summary of kinetic data.

Ligand	k_{obs} (x 10^{-3} s^{-1})	
	buffer pH 5.8	MeOH
DOTA	33.9 ± 1.0	5.62 ± 2.22
DO3A	5.90 ± 0.8	no reaction

For both ligands, complexation was kinetically unfavorable in MeOH in comparison with buffer. These results are in contrast with that of recent studies (Pérez-Malo *et al.* 2018) which report that addition of organic solvent increases the rate of complexation. Hence, water plays an important role in ligand deprotonation of the monoprotonated species, the rate-determining step of the complexation process (Pérez-Malo *et al.* 2018).

Furthermore, isothermal titration calorimetry (ITC) was used to compare the thermodynamics of Gd(DOTA)$^{-}$ formation in these two solvents (O'Brien *et al.* 2015). The negative peaks of the isotherm for the titration of DOTA with Gd^{3+} in MeOH suggests that the binding reaction in MeOH is enthalpy-driven, in contrast with that in buffer (Appendix Fig. 4). In addition, though the calculated ΔG values in both solvents have comparable magnitudes, the $-T\Delta S$ values indicate that the complexation reaction in buffer is entropy-driven. Interestingly, the Wiseman plots (Appendix Fig. 5) suggest that while the metal-to-ligand (M/L) stoichiometry (N) of the resulting complex in buffer is 1:1, the data suggests that the stoichiometry in MeOH is 1:2 (Table 2).

Table 2. Computed global thermodynamic properties (25 °C) for Gd^{3+}-DOTA binding reaction in buffer (pH 5.8) and MeOH.

Property	buffer (pH 5.8)	MeOH
ΔH (kcal/mol)	4.88 ± 0.02	–28.4 ± 10.1
$-T\Delta S$ (kcal/mol)	–14.2 ± 0.00	20.2 ± 10.3
ΔG (kcal/mol)	–9.28 ± 0.57	–8.19 ± 0.14
N	1.07 ± 0.01	0.35 ± 0.16

In contrast to buffer, the negative value for ΔH in MeOH suggests that the solvent molecules are not as strongly bound to the metal ion, as MeOH is a relatively weaker Lewis base than water (Rochester 1972) thereby favoring direct interaction of DOTA with Gd^{3+}. Furthermore, though complexation is an endothermic process in buffer, the reaction ultimately progresses due to the increased entropy caused by the displacement of strongly-bound water molecules in forming the highly-ordered complex (*i.e.*, the chelate effect). In contrast, the relatively weak affinity of MeOH towards Gd^{3+} ion results in a greater ordering of solvent molecules upon displacement, having a greater affinity for themselves. With respect to the

difference in observed stoichiometry (*N*) under these two solvents, it has been previously reported that complexation in a high-donor number solvent (*i.e.*, stronger Lewis base) tends to form 1:1 M/L complexes, while complexation in low-donor number solvents deviate from this ratio (Rounaghi *et al.* 2010).

In summary, kinetic and thermodynamic measurements of Gd(DOTA)$^{-}$ complexation highlight the role of the solvent in the reaction. In particular, slower kinetics was observed in pure MeOH in comparison with buffer, indicating that water plays a role in the complexation process. Of note as well is that the calculated thermodynamic properties suggest that complexation can occur via different mechanisms depending on solvent polarity.

ACKNOWLEDGMENTS

We would like to acknowledge Dr. Evangeline C. Amor for the use of the ThermoScientific MultiSkan™ UV-vis spectrophotometer, as well as Dr. Ricky B. Nellas for the use of the Malvern® Microcal PEAQ-ITC for the isothermal titration calorimetry measurement.

STATEMENT ON CONFLICT OF INTEREST

There are no conflicts to declare.

NOTES ON APPENDICES

The complete appendices section of the study can be accessed at http://philjournsci.dost.gov.ph

REFERENCES

BELLEZA OJV, NARAGA AMB, VILLARAZA AJL. 2018. Relative ligand exchange rates in Gd-based MRI contrast agent formation as probed by Gd-XO complex. J Chin Chem Soc 65: 561–566.

GARCIA J, LIU SZ, LOUIE AY. 2017. Biological effects of MRI contrast agents: Gadolinium retention, potential mechanisms and a role for phosphorus. Phil Trans R Soc A 375: 20170180.

JOB P. 1928. Formation and stability of inorganic complexes in solution. Ann Chim Appl 9: 113–203.

NATRAJAN LS, VILLARAZA AJL, KENWRIGHT AM, FAULKNER S. 2009. Controlled preparation of a heterometallic lanthanide complex containing different lanthanides in symmetrical binding pockets. Chem Commun 6020–22.

O'BRIEN LC, ROOT HB, WEI CC, JENSEN D, SHABESTARY N, DE MEO C, EDER DJ. 2015. M^{2+}•EDTA binding affinities: A modern experiment in thermodynamics for the physical chemistry laboratory. J Chem Educ 92: 1547–51.

PÉREZ-MALO M, SZABÓ G, EPPARD E, VAGNER A, BRÜCHER E, TÓTH I, MAIOCCHI A, SUH EH, KOVÁCS Z, BARANYAI Z, RÓSCH F. 2018. Improved efficacy of synthesizing M^{III}-labeled DOTA complexes in binary mixtures of water and organic solvents: A combined radio- and physicochemical study. Inorg Chem 57: 6107–17.

ROCHESTER CH. 1972. The ionic products of water and methanol in methanol-water mixtures. J Chem Soc Dalton Trans 5–8.

ROUNAGHI GH, SOORGI MH, KAZEMI MS. 2010. Effect of non-aqueous solvents on stoichiometry and selectivity of complexes formed between 4′-nitrobenzo-15-crown-5 with Fe^{3+}, Y^{3+}, Cd^{2+}, Sn^{4+}, Ce^{3+} and Au^{3+} metal cations. Russ J Inorg Chem 55: 355–360.

SUAZO KFG, VILLARAZA AJL. 2015. Gd-XO: A colourimetric probe for the complexation of Gd^{3+} with DO3A-type ligands. Anal Methods 7: 8967–69.

APPENDIX

General Methods

Gadolinium triflate ($Gd(OTf)_3$, Sigma-Aldrich); xylenol orange (XO) disodium salt (Sigma-Aldrich); sodium hydroxide (NaOH, Ajax Finechem); 1,4,7,10-tetraazacyclododecane-1,4,7,10-tetraacetic acid (DOTA, Macrocyclics); and 1,4,7,10-tetraazacyclododecane-1,4,7-triacetic acid (DO3A, Macrocyclics) were purchased as dry solids. Distilled water, glacial acetic acid (HOAc, Ajax Finechem), and methanol (MeOH, J.T. Baker) were procured as liquids. All spectrophotometric studies were conducted using a Thermo Scientific™ Multiskan™ GO microplate spectrophotometer. Isothermal titration calorimetric measurements were conducted using a Malvern® Microcal PEAQ-ITC.

Preparation of Stock Solutions

A solution of 50 mM sodium acetate (NaOAc) buffer with pH = 5.80 was prepared by diluting 2.87 mL HOAc in distilled water (H_2O) and adjusting the pH to 5.80 using 1 M NaOH. The final solution was then diluted to 1 L with H_2O. Another solution of the buffer was prepared at 10 mM concentration with the same pH by diluting 0.287 mL HOAc in H_2O with similar subsequent dilutions and pH adjustments. The final solution was then diluted to 500 mL with H_2O. All $Gd(OTf)_3$, XO, and ligand solutions and dilutions for spectrophotometric measurements were prepared in 50 mM acetate buffer and MeOH. Meanwhile, all solutions and dilutions for ITC measurements were prepared in 10 mM acetate buffer and MeOH.

All 500 and 100 μM ligand solutions were prepared by weighing DOTA (6.4 and 1.3 mg) and DO3A (5.6 and 1.1 mg). They were dissolved in acetate buffer, analytically transferred to 25-mL volumetric flasks, and finally diluted to mark. The same method was used in preparing 100 μM ligand solutions of DOTA and DO3A in MeOH, except that the ligands were dissolved in MeOH. Meanwhile, 800 and 500 μM $Gd(OTf)_3$ solutions were prepared by weighing 11.8 and 7.4 mg, respectively. These were dissolved in acetate buffer, analytically transferred to 25-mL volumetric flasks, and finally diluted to mark. The same method was used in preparing 500 μM $Gd(OTf)_3$ in MeOH except that $Gd(OTf)_3$ was dissolved in MeOH. Subsequently, 50 μM $Gd(OTf)_3$ solutions were prepared by diluting 2.5 mL of 500 μM $Gd(OTf)_3$ solutions in 25-mL volumetric flasks. Lastly, 500 μM XO solutions were prepared by weighing 9.0 mg XO. They were dissolved in acetate buffer, analytically transferred to 25-mL volumetric flasks, and finally diluted to mark. The same method was done in preparing 500 μM XO in MeOH except that XO was dissolved in MeOH. All 50 μM $Gd(OTf)_3$ solutions were prepared by diluting 2.5 mL of 500 μM $Gd(OTf)_3$ solutions in 25-mL volumetric flasks.

Visible Spectra of Xylenol Orange and Gadolinium-Xylenol Orange Solutions in MeOH

Based on a previously described method (Belleza & Villaraza 2014) with slight modifications, 25 μM of GdXO in MeOH solution was prepared by mixing equal volumes (3 mL) of 50 μM XO and 50 μM $Gd(OTf)_3$, using MeOH as solvent. Once a uniform color was achieved after mixing, the UV-Vis absorption spectra of the test solutions were recorded using quartz cuvettes (blank solution: MeOH). The visible spectra of the solutions were recorded at 300–800 nm.

Determination of Gd-XO Complex Stoichiometry by Job's Method of Continuous Variation: Effect of Solvent

Job plots were constructed as previously described (Belleza & Villaraza 2014) to determine Gd-XO stoichiometry in MeOH. Solutions of increasing mole fractions of Gd^{3+} ions were prepared in vials by mixing different volumes of 50 μM $Gd(OTf)_3$ solution and 50 μM stock XO in MeOH, keeping the sum of the concentrations constant (Table 1).

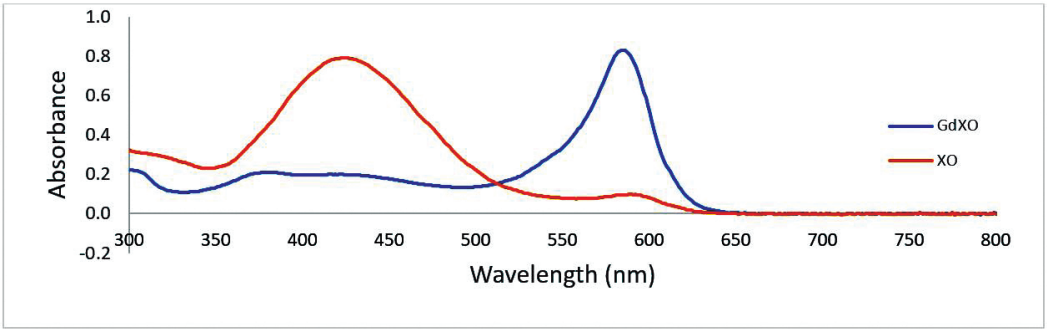

Figure 1. Absorption spectra of XO and GdXO complex in MeOH. Maximum absorbance for XO and GdXO in MeOH were recorded at 436 nm and 582 nm.

Table 1. Composition of test solutions in the determination of Gd-XO complex stoichiometry.

Solution No.	Mole Fraction	$V_{Gd(OTf)3}$ (mL)	V_{XO} (mL)	$V_{solvent}$ (mL)
1	0	0	6.0	1.0
2	0.1	0.6	5.4	1.0
3	0.2	1.2	4.8	1.0
4	0.3	1.8	4.2	1.0
5	0.4	2.4	3.6	1.0
6	0.5	3.0	3.0	1.0
7	0.6	3.6	2.4	1.0
8	0.7	4.2	1.8	1.0
9	0.8	4.8	1.2	1.0
10	0.9	5.4	0.6	1.0
11	1.0	6.0	0	1.0

Figure 2. Solutions formed from increasing Gd^{3+} mole fraction with XO, starting from $x_{Gd3+} = 0$ to $x_{Gd3+} = 1.0$(increment: $x_{Gd3+} = +0.1$).

The absorbance spectra from 300 to 800 nm of the solutions (Fig. 2) were obtained, and the absorbance maxima noted (blank solution: MeOH). The Job's plot was constructed by plotting absorbance as a function of mole fraction, and the stoichiometry of the complex determined from the plot maxima using the formula x = (1–*X*)/*X* where *X* is the mole fraction at which maximum absorbance occurs and x is the integer corresponding to the stoichiometry of Gd-XO complex.

Ligand Exchange Kinetics

Ligand exchange kinetics was investigated as previously described (Belleza *et al.* 2018) with slight modifications. The blank solutions used were the previously prepared 50 mM acetate buffer and MeOH, depending on the system under investigation. The 750 µL volumes of 50 µM $Gd(OTf)_3$ and 50 µM XO were equilibrated with the cell temperature (25 °C). Two 750-µL aliquot of 500 µM of ligand solutions (*i.e.*, ligand in 20-fold excess) were added to the Gd-XO solution and changes in the absorption spectra were monitored (Fig. 3) after addition with a lag time of eight (8) seconds (blank solutions: MeOH and acetate buffer). The rate constants of each ligand exchange system were estimated using the least-squares approximation method. All measurements were made in two trials with two replicates for each trial.

Isothermal Titration Calorimetry Measurements

ITC measurements were performed as previously described (O'Brien *et al.* 2015). Initialization parameters used throughout the runs are specified in Table 2. The sample cell was initially filled with 300 µL of 100 µM ligand solution. The titrant used for all ITC measurements was 800 µM $Gd(OTf)_3$ (reference cell: double-distilled water). Isotherms (Fig. 4) were treated for their corresponding Wiseman plots using the MicroCal PEAQ-ITC Control Software (Fig. 5). Two trials were performed per solvent.

Table 2. ITC initialization parameters.

Temperature (°C)	25.0
Number of Injections	19
Volume of Titrant During Initial Injection (µL)	0.4
Volume of Titrant per Injection (µL)	3.0
Reference Power (µcal/s)	10.0
Feedback	High
Stir Speed (rpm)	750
Initial Delay (s)	60
Injection Spacing (s)	150
Injection Duration (s)	4.0

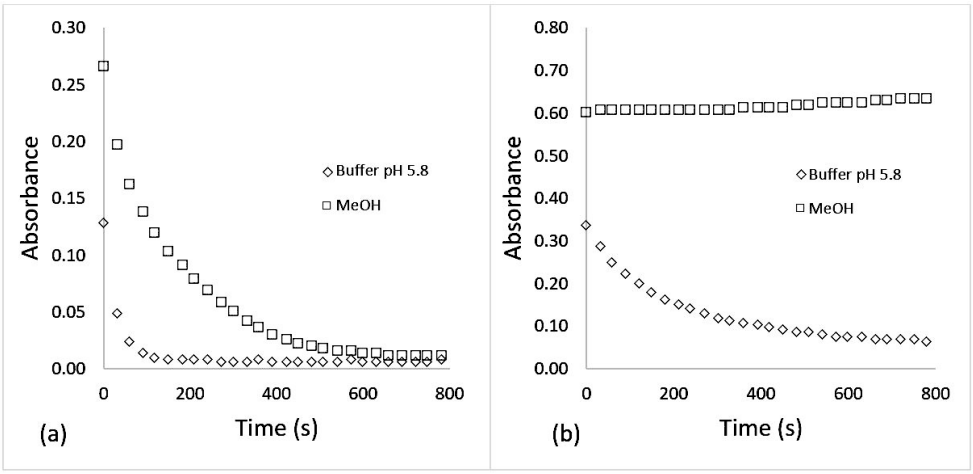

Figure 3. Normalized kinetic decay curves of Gd-XO complex upon (a) DOTA and (b) DO3A competition in acetate buffer and MeOH. All starting concentration used in MeOH were half of that used in acetate buffer due to solubility issues of the ligands.

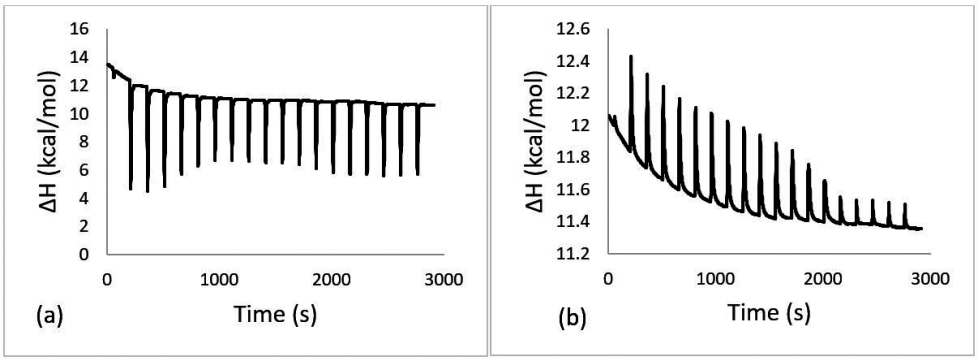

Figure 4. Representative ITC isotherms of Gd^{3+} binding with DOTA in (a) MeOH and (b) acetate buffer.

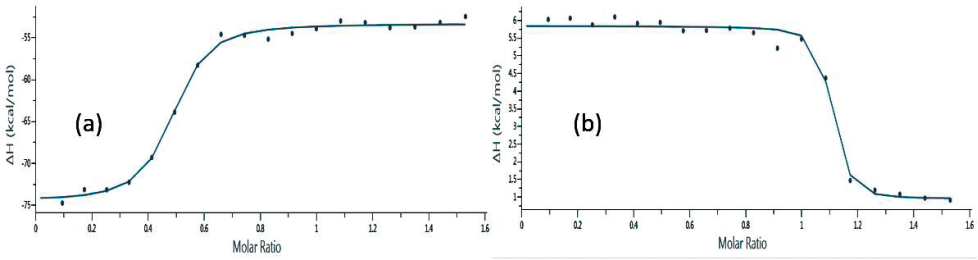

Figure 5. Wiseman plots of Gd^{3+} complexation with DOTA in (a) MeOH and (b) acetate buffer pH 5.8.

REFERENCES

BELLEZA OJV, VILLARAZA AJL. 2014. Ion charge density governs selectivity in the formation of metal-xylenol orange (M-XO) complexes. Inorg Chem Commun 47: 87–92.

BELLEZA OJV, NARAGA AMB, VILLARAZA AJL. 2018. Relative ligand exchange rates in Gd-based MRI contrast agent formation as probed by Gd-XO complex. J Chin Chem Soc 65: 561–566.

JOB P. 1928. Formation and stability of inorganic complexes in solution. Ann Chim Appl 9: 113–203.

O'BRIEN LC, ROOT HB, WEI CC, JENSEN D, SHABESTARY N, DE MEO C, EDER DJ. 2015. M^{2+}•EDTA binding affinities: A modern experiment in thermodynamics for the physical chemistry laboratory. J Chem Educ 92: 1547–51.